

# Contrasting effects of cyclophosphamide on anti-CTL-associated protein 4 blockade therapy in two mouse tumor models

Yuichi Iida,<sup>1</sup> Nanae Harashima,<sup>1,2</sup> Takanobu Motoshima,<sup>3</sup> Yoshihiro Komohara,<sup>4</sup>  Masatoshi Eto<sup>5</sup> and Mamoru Harada<sup>1</sup> 

<sup>1</sup>Department of Immunology, Faculty of Medicine, Shimane University, Shimane; <sup>2</sup>Laboratory of Biometabolic Chemistry, Faculty of Medicine, School of Health Sciences, University of Ryukyus, Okinawa; Departments of <sup>3</sup>Urology; <sup>4</sup>Cell Pathology, Graduate School of Medical Science, Kumamoto University, Kumamoto; <sup>5</sup>Department of Urology, Graduate School of Medical Science, Kyushu University, Fukuoka, Japan

## Key words

Anti-CTLA-4 therapy, CCL2, cyclophosphamide, IL-6, MDSC

## Correspondence

Mamoru Harada, Department of Immunology, Shimane University Faculty of Medicine, Izumo, Shimane 693-8501, Japan.

Tel./Fax: +81-853-20-2150;

E-mail: haramamo@med.shimane-u.ac.jp

## Funding Information

JSPS KAKENHI, (17K07217); The Shimane University "SUIGANN" Project.

Received May 25, 2017; Revised July 27, 2017; Accepted July 29, 2017

*Cancer Sci* 108 (2017) 1974–1984

doi: 10.1111/cas.13337

Immune checkpoint blockade is a promising anticancer therapy, but must be used in combination with other anticancer therapies to increase its therapeutic efficacy. Cyclophosphamide (CP) is a chemotherapeutic drug that shows immune-modulating effects. In this study, we examined the effect of CP on anti-CTL-associated protein 4 (CTLA-4) blockade therapy in two mouse tumor models. Drastic tumor regression was observed in the CT26 colon carcinoma model after i.p. injection of CP (100 mg/kg) followed by anti-CTLA-4 antibody. However, administration in the reverse order increased apoptosis in tumor-specific CD8<sup>+</sup> T cells. In the RENCA renal carcinoma model, the antitumor effect of combination therapy was marginal and the tumor-bearing state reduced body weight with an increased serum level of interleukin-6. Interestingly, although CP monotherapy increased myeloid-derived suppressor cells (MDSCs) in the spleens of both models, subsequent anti-CTLA-4 therapy increased MDSCs only in RENCA-bearing mice. Additionally, the serum levels of chemokine ligand 2 and C-X-C motif chemokine 10 were increased by the combination therapy only in RENCA-bearing mice and *in vivo* depletion of Gr-1<sup>+</sup> cells augmented the antitumor effect to some degree. These results reveal a contrasting effect of CP on anti-CTLA-4 therapy between the two mouse tumor models. Cyclophosphamide augments the antitumor effect of anti-CTLA-4 therapy in CT26-bearing hosts, whereas CP after anti-CTLA-4 therapy attenuates this effect through induction of apoptosis in tumor-reactive T cells. Alternatively, CP-induced MDSCs can be increased by anti-CTLA-4 therapy only in RENCA-bearing hosts with an elevated level of interleukin-6.

Immune checkpoint blockade therapy targeting CTLA-4 or PD-1/PD-L1 has been considered a promising anticancer therapy.<sup>(1,2)</sup> Although the therapeutic efficacy of ICB has been reported in several types of cancers, several issues remain to be addressed. First, its therapeutic efficacy has been observed in approximately 20% of patients; the majority of patients show no definite response.<sup>(3)</sup> Accordingly, there is an urgent need to expand the proportion of patients that respond to ICB therapy or its combination with other anti-cancer therapies.<sup>(4,5)</sup> Another issue associated with ICB is IrAEs. Immune checkpoint blockade therapy is commonly associated with IrAEs, such as autoimmune disease.<sup>(5,6)</sup> Given that ICB therapy takes the brake off T cell immunity,<sup>(7)</sup> a therapy-associated risk of IrAEs is inevitable. Thus far, clinical treatment for ICB therapy-associated IrAEs involves inhibiting inflammatory and immune responses. However, this supportive care could exert negative effects on the therapeutic efficacy of ICB therapy.

Several chemotherapeutic drugs show immune-modulating effects.<sup>(8)</sup> Anticancer drugs such as anthracyclines induce cancer cell death and promote the uptake of dying tumor cells and the processing of tumor antigens by DCs.<sup>(9)</sup> This immunogenic

cancer cell death is crucial for treatment-associated prognosis and for the survival of tumor-bearing hosts. Other chemotherapeutic drugs modulate immune responses. The alkylating agent CP is a representative immune-modulating drug that diminishes the functionality of Tregs while maintaining immune competence when given at low/medium doses.<sup>(10,11)</sup> Cyclophosphamide also induces immunogenic cancer cell death and, at higher doses, lymphopenia accompanying a cytokine storm.<sup>(10)</sup> Other chemotherapeutic drugs, such as gemcitabine and 5-fluorouracil, decrease immunosuppressive MDSCs.<sup>(12,13)</sup> Therefore, many researchers have aimed to determine the optimal combination of chemotherapeutic drugs and ICB therapy.<sup>(3,7)</sup> However, one important aspect to remember is that chemotherapeutic drugs can destroy proliferating cancer cells as well as immune cells. Given that ICB therapy exerts antitumor effects through reactivation of exhausted antitumor T cells, subsequent CP treatment could abolish vigorously proliferating antitumor T cells after ICB therapy.

In this study, we examined the antitumor effects induced by combining CP and anti-CTLA-4 blockade therapy using two

murine tumor models: the immunogenic CT26 colon carcinoma model and the non/low immunogenic RENCA renal carcinoma model. In the CT26 model, T cell-dependent tumor regression was observed following i.p. injection of CP (100 mg/kg) on day 12 followed by i.p. injection of anti-CTLA-4 antibody on days 13 and 15. However, this antitumor effect was attenuated when the order was reversed, with increased apoptosis in tumor-specific CD8<sup>+</sup> T cells in the draining LNs. In contrast, the combination therapy-induced antitumor effects were marginal in the RENCA model and the RENCA-bearing state was associated with increased serum levels of IL-6, as well as a reduction in body weight. Interestingly, this combination therapy significantly increased the serum levels of CCL2 and CXCL10 only in RENCA-bearing mice. Furthermore, CP monotherapy significantly increased MDSCs in both tumor models, whereas the following anti-CTLA-4 therapy escalated these CP-induced MDSCs only in RENCA-bearing hosts. These results reveal contrasting effects of CP on anti-CTLA-4 blockade therapy in two mouse tumor models.

## Materials and Methods

**Mice and tumor cell lines.** BALB/c and C57BL/6 female mice (6–7 weeks old) were purchased from CLEA Japan (Tokyo, Japan). Mice were maintained under specific pathogen-free conditions. Experiments were carried out according to the ethical guidelines for animal experiments of the Shimane University Faculty of Medicine (IZ26-248, IZ27-145) (Shimane, Japan). CT26 is a colon carcinoma cell line and RENCA is a renal cell carcinoma cell line. Both cell lines are of BALB/c mouse origin. B16 melanoma is of C57BL/6 mouse origin. All cell lines were maintained in RPMI-1640 Medium (Sigma-Aldrich, St. Louis, MO, USA) supplemented with 10% FBS and 20 µg/mL gentamycin (Sigma-Aldrich).

**Dose-dependent effects of CP *in vivo*.** BALB/c mice received an s.c. injection of  $5 \times 10^5$  tumor cells in the right flank. On day 12, mice received an i.p. injection of 50, 100, 200, or 300 mg/kg CP (Shionogi, Osaka, Japan) or PBS as a control. Thereafter, tumor size (mm<sup>2</sup>) and body weight were measured on the indicated days.

**Treatment protocol.** BALB/c mice were injected s.c. with  $5 \times 10^5$  tumor cells in the right flank and received an i.p. injection of 100 mg/kg CP and/or an i.p. injection of anti-CTLA-4 mAb (100 µg) on the indicated days. Anti-CTLA-4 mAb was prepared from the supernatants of hybridoma UC10-4F10-7, which was purchased from ATCC (Rockville, MD, USA). The same volume of hamster IgG (100 µg) (Alpha Diagnostic International, San Antonio, TX, USA) was injected as a control. In some experiments, CT26-bearing mice received an i.p. injection of 100 mg/kg CP and/or an i.p. injection of anti-PD-1 mAb (100 µg) (RMP 1-14; Bio X Cell, West Lebanon, NH, USA) on the indicated days. The same volume of rat IgG (100 µg) (Sigma-Aldrich) was injected as a control. Thereafter, tumor size (mm<sup>2</sup>) and body weight were measured on the indicated days.

***In vivo* depletion of immune cells.** To deplete CD4<sup>+</sup> or CD8<sup>+</sup> T cells, 100 µg anti-CD4 mAb (GK1.4; eBioscience, San Diego, CA, USA) or anti-CD8 mAb (53-6.72; eBioscience) were given i.p. on days 14 and 16 after tumor inoculation. To deplete MDSCs, 100 µg anti-Gr-1 mAb (RB6-8C5; Cedarlane Laboratory, Burlington, NC, USA) was injected i.p. on days 15 and 17. The same volume of rat IgG was injected as a control.

**Flow cytometry.** To assess the frequency of tumor-specific CTLs, PE-conjugated tetramer of an H-2L<sup>d</sup>-binding peptide

(SPSYVYHQF) was used, which is derived from the envelope protein (gp70) of an endogenous murine leukemia virus. It is a CT26-associated tumor-derived peptide<sup>(14)</sup> and is designated AH1 in the current study. The tetramer was purchased from MBL (Nagoya, Japan). Measles virus hemagglutinin (SPGRSFSYF) was used as an H-2L<sup>d</sup>-binding control peptide. All peptides were >80% pure and were purchased from Invitrogen (Grand Island, NY, USA). On day 23 after tumor inoculation (7 days after the last therapy), spleen cells were cultured *in vitro* with AH1 peptide (10 µg/mL) in the presence of IL-2 (20 U/mL) for 4 days. Thereafter, the cultured cells were stained with FITC-conjugated anti-CD8 mAb (Southern Biotech, Birmingham, AL, USA) and analyzed on a FACSCaliber flow cytometer (Becton-Dickinson, Franklin Lakes, NJ, USA). To assess the cellular subsets of the spleen, the cell suspension was treated with red blood cell-lysing buffer, stained with the indicated mAbs, and analyzed by flow cytometry. The following mAbs were used for staining: APC-conjugated anti-CD45 (BioLegend, San Diego, CA, USA), PE-conjugated anti-CD11b (BioLegend), FITC-conjugated anti-Gr-1 (R&D Systems, Minneapolis, MN, USA), and PE/cy7-conjugated anti-Ly6C (BioLegend). To examine Tregs, the cell suspension was stained with APC-conjugated anti-CD45 (BioLegend) and PE-conjugated anti-CD4 (AbD Serotec, Oxford, UK). After fixing with IntraPrep Permeabilization Reagent (Beckman Coulter, Brea, CA, USA), cells were stained with FITC-conjugated anti-Foxp3 mAb (Santa Cruz Biotechnology, Santa Cruz, CA, USA). To examine apoptotic cells in the AH1 peptide-specific CD8<sup>+</sup> T cell subset, cells were first stained with FITC-conjugated anti-CD8 mAb and the PE-conjugated AH1 tetramer (MBL) followed by APC-conjugated annexin V (BD Pharmingen, Tokyo, Japan). To examine PD-L1 expression, CT26 cells were stained with anti-PD-L1 mAb (rat IgG, 10F.9F2; BioLegend) or rat IgG followed by FITC-conjugated goat anti-rat IgG (Abcam, Cambridge, UK). Analysis was performed on the FACSCaliber.

**Cytotoxicity assays.** On day 23 after tumor inoculation (7 days after the last therapy), spleen cells were cultured *in vitro* with AH1 peptide (10 µg/mL) in the presence of IL-2 (20 U/mL) for 4 days. Thereafter, cytotoxicity was measured using a 5-h <sup>51</sup>Cr-release assay.

**Enzyme-linked immunosorbent assay.** Levels of IL-6 and TNF-α in culture supernatants and the sera were determined using an ELISA Development Kit (PeproTech, Rocky Hill, NJ, USA).

**Proteome profiler cytokine array.** To evaluate the levels of a panel of cytokines and chemokines, sera were analyzed using the Proteome Profiler Mouse Cytokine Array (R&D Systems) according to the manufacturer's protocol. For the analyses, 300-µL sera samples were used. Densitometric analyses were carried out using ImageJ software (<http://rsb.info.nih.gov/ij/>).

**Statistical analysis.** Data were analyzed using unpaired two-tailed Student's *t*-test (between two groups) or ANOVA with Tukey's post hoc test (among more than two groups). A *P*-value < 0.05 was considered statistically significant.

## Results

**Dose-dependent effects of CP on tumor size and body weight in CT26-bearing mice.** We first examined the dose-dependent effects of CP on tumor size and body weight in CT26-bearing mice. Cyclophosphamide was introduced by i.p. injection on day 12 at doses of 50, 100, 200, and 300 mg/kg. Injection of CP (50 mg/kg) suppressed tumor growth, albeit not

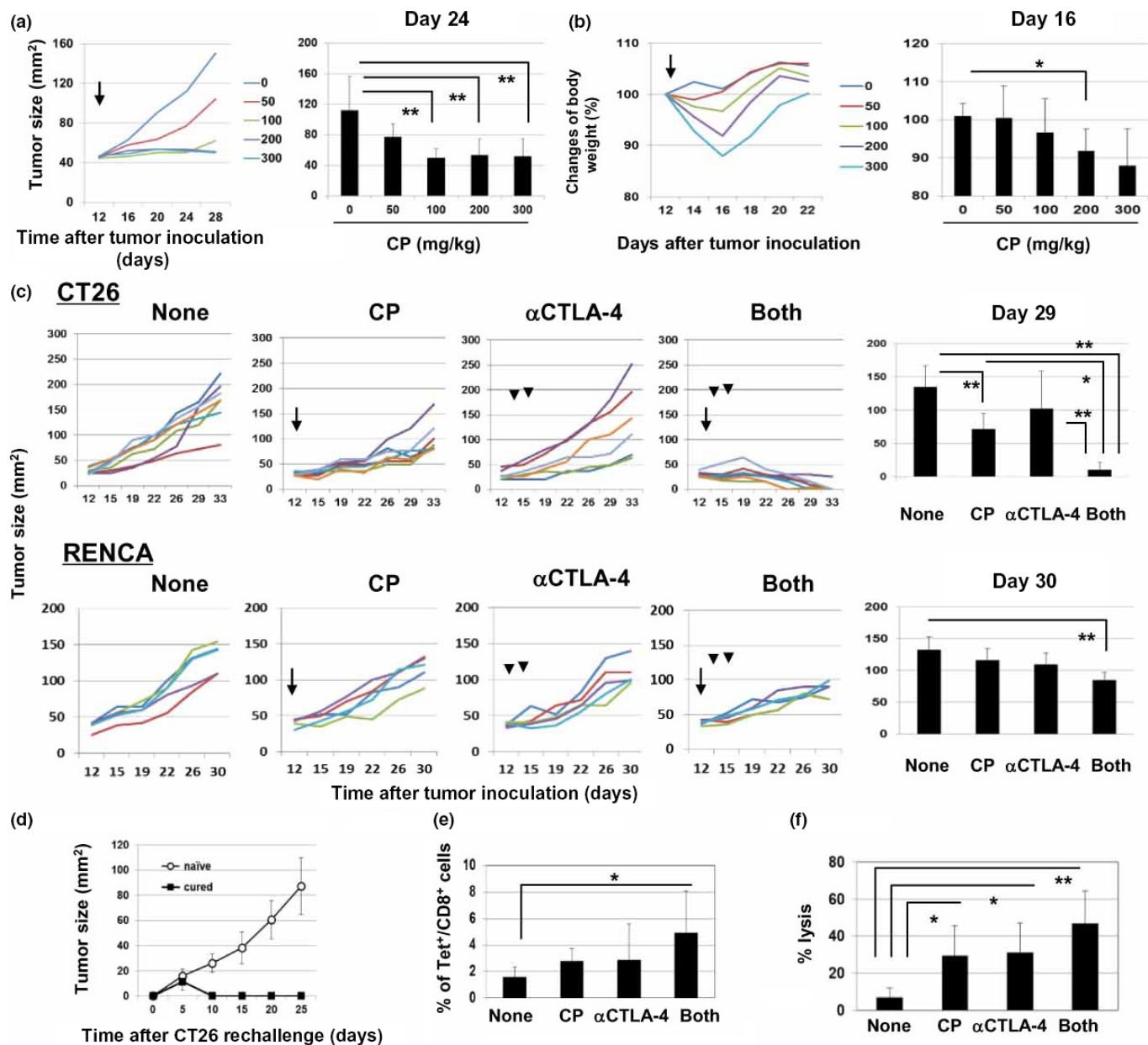


**Fig. 1.** CD8<sup>+</sup> T cell-dependent regression of established CT26 colon carcinoma cells following cyclophosphamide (CP) and anti-CTLA-4 therapy. (a,b) BALB/c mice were inoculated with CT26 cells ( $5 \times 10^5$ ) by s.c. injection and on day 12, CP was introduced by i.p. injection at 50, 100, 200, or 300 mg/kg. Thereafter, tumor size and body weight were measured. Arrows indicate the times of CP injection ( $n = 6$  or  $7$ ). Data from day 24 (tumor size) and day 16 (body weight) are presented as means  $\pm$  SD. \* $P < 0.05$ , \*\* $P < 0.01$  (ANOVA). (c) BALB/c mice were inoculated s.c. with CT26 cells ( $5 \times 10^5$ ) or RENCA cells ( $1 \times 10^6$ ). Twelve days after tumor inoculation, mice received an i.p. injection of CP (100 mg/kg) followed by an i.p. injection of anti-CTLA-4 mAb (100  $\mu$ g) on days 13 and 15. As a control, hamster IgG was administered i.p. Line graphs: arrows represent the timing of CP injection and arrowheads represent the timing of anti-CTLA-4 therapy ( $n = 5$  or  $7$ ). Column graphs: data from day 29 or 30 are presented as the mean  $\pm$  SD. Similar results were obtained from three independent experiments. \* $P < 0.05$ , \*\* $P < 0.01$  (ANOVA). (d) CT26-cured BALB/c mice that received the combination therapy were inoculated with s.c. with  $2.5 \times 10^5$  cells 3 months after the last therapy. Naive mice were also inoculated with CT26 cells ( $n = 5$ ). (e) On day 18 after CT26 inoculation, the spleens were harvested and cultured with AH1 peptide in the presence of interleukin (IL)-2 (20 U/mL) for 4 days. *In vitro*-stimulated spleen cells were stained with FITC-conjugated anti-CD8 mAb and the phycoerythrin-conjugated AH1 tetramer. The percentage of tetramer<sup>+</sup> cells among CD8<sup>+</sup> T cells was calculated ( $n = 4$ ). \* $P < 0.05$  (ANOVA). (f) Cytotoxicity of the cultured cells against CT26 cells was examined using a 5-h <sup>51</sup>Cr-release assay at a ratio of 50:1 ( $n = 5$ ). \* $P < 0.05$ , \*\* $P < 0.01$  (ANOVA).

significantly. Injection of CP at 100, 200, or 300 mg/kg suppressed tumor growth similarly (Fig. 1a). However, weight loss was more severe when CP was injected at a dose of 200 or 300 mg/kg than when injected at a dose of 100 mg/kg (Fig. 1b). These results indicate that 100 mg/kg CP exerted a comparable antitumor effect with less weight loss. We also examined the effect of 100 mg/kg CP on Tregs in CT26-

bearing mice (Fig. S1). Although i.p. injection of CP (100 mg/kg) on day 12 did not change the percentages of CD4<sup>+</sup> Foxp3<sup>+</sup> Tregs among CD45<sup>+</sup> cells in tumor sites, this treatment decreased the percentages of tumor-infiltrating CD45<sup>+</sup> immune cells, thereby resulting in a significant decrease in the percentages of Tregs in tumor sites (Fig. S1b). Based on these results, we judged that 100 mg/kg CP was the optimal dose for use in

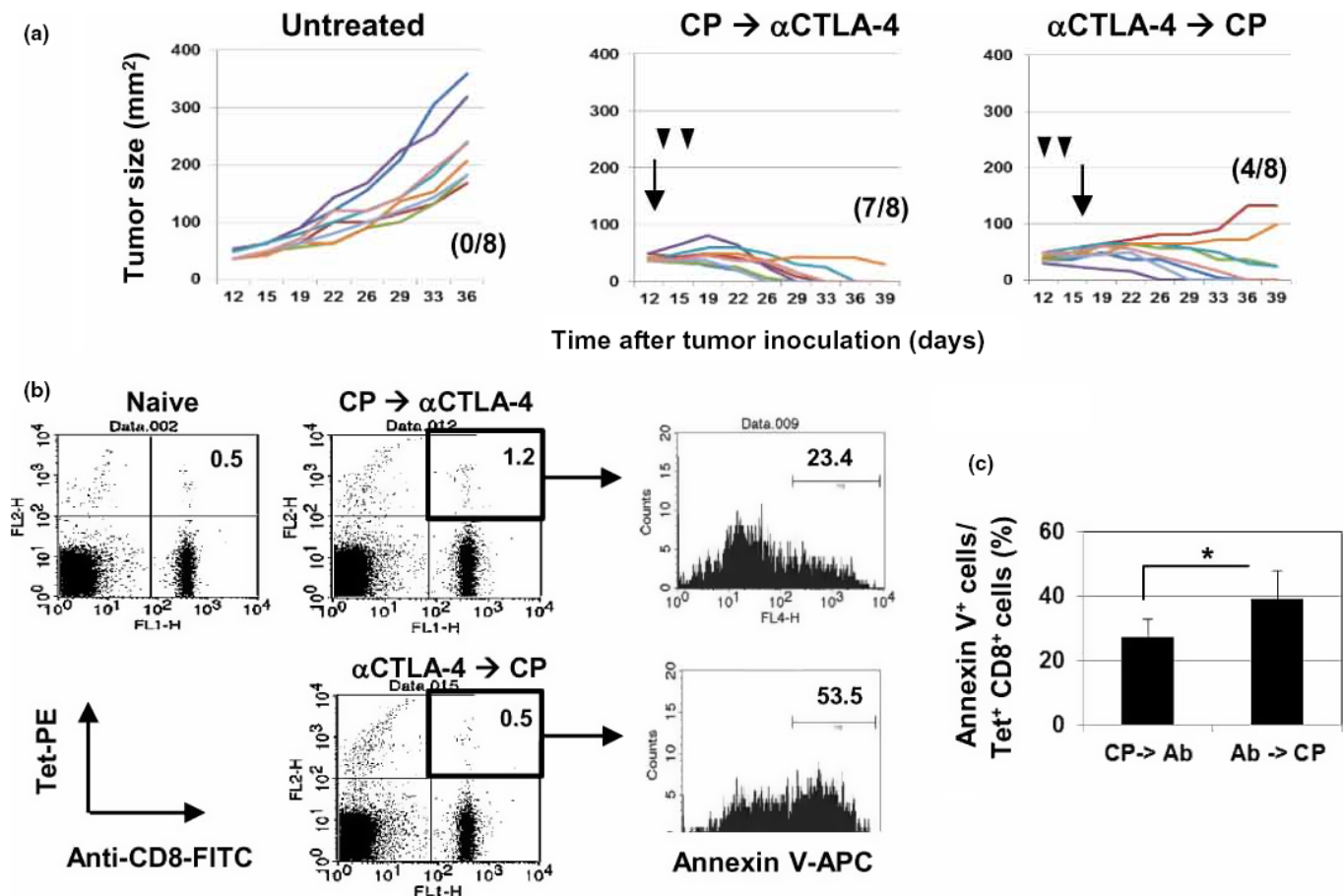


**Fig. 2.** Cyclophosphamide (CP) after anti-CTLA-4 therapy attenuates antitumor effects through the induction of apoptosis in tumor-specific T cells. (a) BALB/c mice were inoculated s.c. with CT26 colon carcinoma cells ( $5 \times 10^5$ ). One group of mice was given CP (100 mg/kg) i.p. on day 12 followed by anti-CTLA-4 mAb (100  $\mu$ g) on days 13 and 15. Another group of mice received anti-CTLA-4 mAb (100  $\mu$ g) on days 12 and 14, and CP (100 mg/kg) on day 15 ( $n = 8$ ). Arrows represent the timing of CP injection; arrowheads represent the timing of anti-CTLA-4 therapy. Hamster IgG was given i.p. as a control. Numbers in parentheses represent cured mice/total mice. (b) Draining lymph nodes were harvested on day 18 after CT26 inoculation. Flow cytometry was carried out after staining with FITC-conjugated anti-CD8 mAb, phycoerythrin (PE)-conjugated AH1 tetramer (Tet), and annexin V–allophycocyanin (APC). Numbers represent percentages. (c) Percentage of annexin V<sup>+</sup> cells in the Tet<sup>+</sup> CD8<sup>+</sup> T-cell subset is presented as the mean  $\pm$  SD ( $n = 4$ ). \* $P < 0.05$  (Student's *t*-test).

combination with ICB therapy and used this dose in the following experiments.

**Antitumor effects induced by CP and anti-CTLA-4 therapy.** We next examined the antitumor effects induced by a combination of CP with anti-CTLA-4 therapy using two syngeneic tumor mouse models, CT26 colon carcinoma and RENCA renal carcinoma (Fig. 1c). Cyclophosphamide (100 mg/kg) was given i.p. on day 12 and anti-CTLA-4 mAb (100  $\mu$ g) was given i.p. on days 13 and 15. In the CT26 model, CP significantly decreased tumor growth, whereas anti-CTLA-4 therapy resulted in varied tumor growth with no statistical significance. However, their combination induced drastic tumor regression in most mice. In the RENCA model, neither CP nor anti-CTLA-4 therapy resulted in any significant antitumor effect. When combined, tumor growth was moderately suppressed compared to that observed in the untreated controls. We also examined the antitumor effects in B16 melanoma-bearing mice. Either CP or anti-CTLA-4 therapy suppressed tumor growth, whereas no additive or synergistic antitumor effects were observed (Fig. S2).

We next determined whether tumor-specific T cells were involved in the combination effects observed in CT26-bearing

mice, because CT26-cured mice showed protective immunity against CT26 at the rechallenge 3 months after the last therapy (Fig. 1d). The antitumor effects were partially and completely abrogated by *in vivo* depletion of CD4<sup>+</sup> T cells and CD8<sup>+</sup> T cells, respectively (Fig. S3a). Spleen cells from CT26-bearing and treated mice on day 18 after tumor inoculation were also examined for their frequency of tumor-specific CD8<sup>+</sup> T cells and anti-CT26 cytotoxicity after *in vitro* stimulation with AH1 peptide, an H-2L<sup>d</sup>-restricted tumor peptide of CT26 carcinoma.<sup>(14)</sup> The combination therapy significantly increased the frequency of AH1 peptide-specific T cells among CD8<sup>+</sup> T cells compared with the untreated group (Figs 1e and S3b). Although monotherapy with either CP or anti-CTLA-4 mAb significantly increased anti-CT26 cytotoxicity compared with the untreated group ( $P < 0.05$ ), their combination further increased these levels ( $P < 0.01$ ) (Figs 1f and S3c).

**Cyclophosphamide after anti-CTLA-4 therapy attenuates the antitumor effects through induction of apoptosis in tumor-specific CD8<sup>+</sup> T cells *in vivo*.** Cyclophosphamide could kill tumor-specific T cells that are vigorously proliferating in response to anti-CTLA-4 therapy. Therefore, we compared the antitumor effects when CP was given either before or after anti-CTLA-4

therapy (Fig. 2a). Cyclophosphamide before anti-CTLA-4 therapy induced drastic CT26 regression in 7 of 8 mice, consistent with the results presented in Figure 1(c), whereas CP after anti-CTLA-4 therapy resulted in fewer cured mice. Although no statistical difference in tumor size was observed between these two regimens (data not shown), CP after anti-CTLA-4 therapy seemed to attenuate the antitumor effects. Therefore, we next examined the frequency of tumor-specific CD8<sup>+</sup> T cells in CT26-bearing and treated mice. Although there was no difference in the percentage of AH1 tetramer<sup>+</sup> CD8<sup>+</sup> T cells in the draining LNs of CT26-bearing mice treated with CP before or after anti-CTLA-4 therapy (data not shown), the percentage of apoptosis increased significantly when CP was given after anti-CTLA-4 therapy (Fig. 2b,c). These results indicate that CP induces apoptosis in tumor-specific CD8<sup>+</sup> T cells that are vigorously proliferating after anti-CTLA-4 therapy in CT26-bearing mice.

We also examined the antitumor effects of CP and anti-PD-1 therapy using the CT26 model. *In vitro*, CT26 cells expressed PD-L1 on the cell surface (Fig. 3a). Although the mean tumor size was smaller in mice treated with CP followed by anti-PD-1 therapy compared with the monotherapy group, the antitumor effects induced by their combination were marginal and no tumor regression was observed (Fig. 3b,c). Cyclophosphamide after PD-1 therapy slightly attenuated the antitumor effects, but not significantly. Together, these results suggest that the immune-modulating effects of CP on anti-PD-1 therapy are not as effective as on anti-CTLA-4 therapy.

**Changes of serum levels of IL-6, TNF- $\alpha$ , CCL2, and CXCL10 in RENCA-bearing mice.** Immune checkpoint blockade therapy is frequently associated with IrAEs,<sup>(5,6)</sup> thus, we measured the body weights of treated mice as an indicator of IrAEs. In RENCA-bearing mice, untreated mice began to lose weight 19 days after tumor inoculation (Fig. 4a). Either CP or anti-CTLA-4 therapy further reduced body weight in RENCA-bearing mice. However, such a tendency was not observed in CT26-bearing or naïve mice. Unexpectedly, the reduction in body weight observed in RENCA-bearing mice appeared to be relieved when CP was given before anti-CTLA-4 therapy. These results suggest that RENCA-bearing mice are more susceptible to tumor-associated weight loss compared with CT26-bearing mice, which is aggravated by anti-CTLA-4 therapy.

Inflammatory cytokines such as IL-6 and TNF- $\alpha$  are responsible for cachexia in tumor-bearing hosts.<sup>(15)</sup> Therefore, we measured their levels both *in vitro* and *in vivo*. RENCA cells produced higher levels of IL-6 and TNF- $\alpha$  relative to CT26 cells *in vitro* (Fig. 4b). In addition, the serum levels of IL-6 were increased in untreated RENCA-bearing mice compared with naïve mice (Fig. 4c). Both CP and anti-CTLA-4 therapy alone significantly decreased the levels of IL-6 in RENCA-bearing mice, and their combination further decreased these levels. Alternatively, although the RENCA-bearing state was associated with increased levels of TNF- $\alpha$ , the difference was not significant. However, either CP or anti-CTLA-4 therapy significantly decreased the level of TNF- $\alpha$ . In contrast, such significant changes were not observed in CT26-bearing mice.

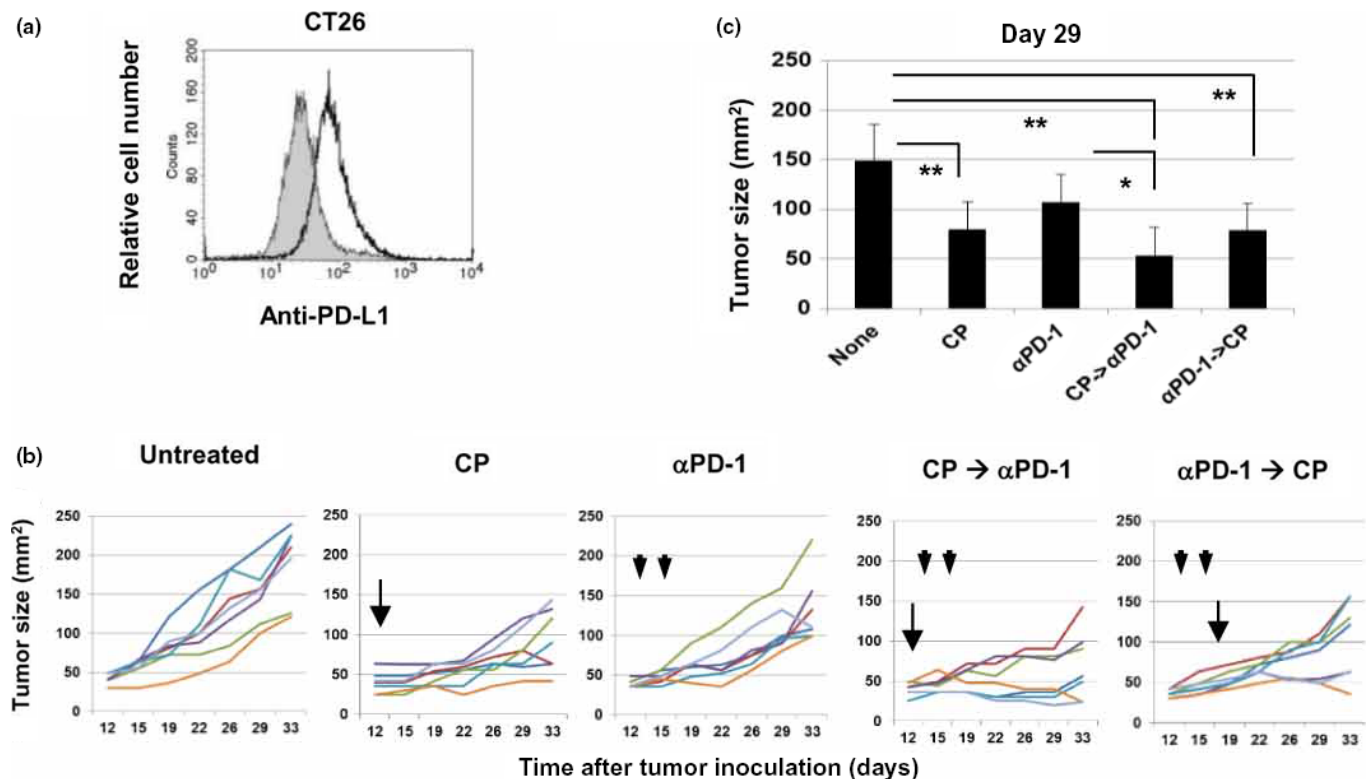


**Fig. 3.** Insufficient antitumor effects of cyclophosphamide (CP) and anti-programmed cell death-1 ( $\alpha$ PD-1) therapy in a CT26 colon carcinoma mouse model. (a) anti-PD-L1 mAb followed by FITC-conjugated anti-rat IgG (bold line). Rat IgG was used as an isotype-matched control (gray background). (b) BALB/c mice were inoculated s.c. with CT26 cells ( $5 \times 10^5$ ). Twelve days after tumor inoculation, mice received CP (100 mg/kg) i.p. followed by anti-PD-1 mAb (100  $\mu$ g) on days 13 and 15. One group of mice received anti-PD-1 mAb (100  $\mu$ g) on days 12 and 14, and CP (100 mg/kg) on day 15. Hamster IgG was given i.p. as a control ( $n = 7$ ). Lines represent tumor growth. Arrows represent the timing of CP injection; arrowheads represent the timing of anti-PD-1 therapy. (c) Data are the results from day 29 and are presented as the mean  $\pm$  SD. \* $P < 0.05$ , \*\* $P < 0.01$  (ANOVA).

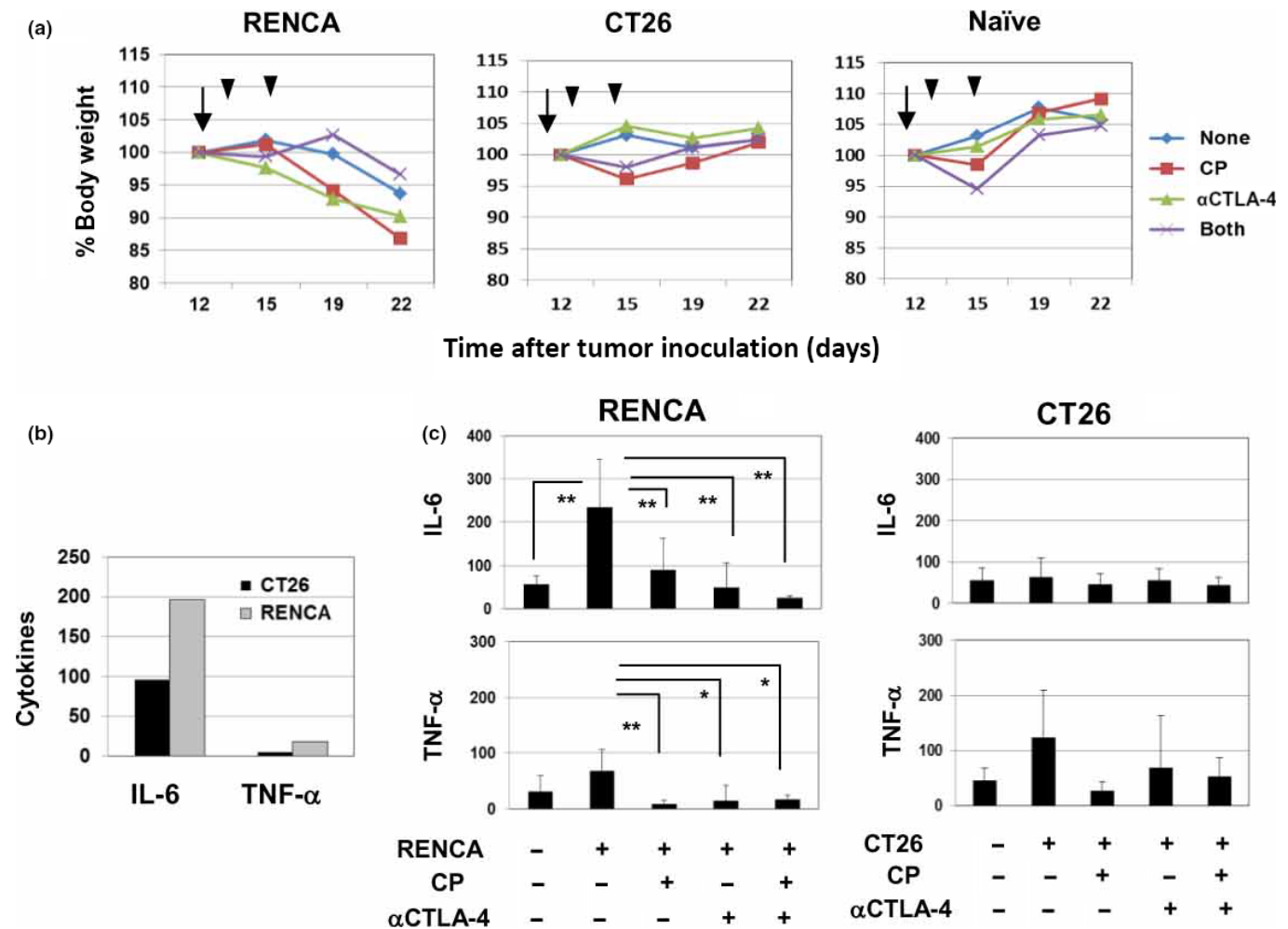


**Fig. 4.** Weight loss and increased levels of interleukin (IL)-6 in RENCA renal carcinoma-bearing mice. (a) BALB/c mice were inoculated s.c. with CT26 colon carcinoma cells ( $5 \times 10^5$ ) or RENCA cells ( $1 \times 10^6$ ) and, on day 12, mice received an i.p. injection of CP (100 mg/kg) followed by an i.p. injection of anti-CTLA-4 mAb (100  $\mu$ g) on days 13 and 15. Body weights were measured thereafter. Data are representative of the means of six mice. Arrows represent the timing of cyclophosphamide (CP) injection; arrowheads represent the timing of anti-CTLA-4 therapy. (b) Levels (pg/mL) of cytokines in the culture supernatants from CT26 colon carcinoma and RENCA cells ( $4 \times 10^4$  cells/mL for 48 h) were measured using ELISA. (c) Sera were collected on day 18 after tumor inoculation and the levels (pg/mL) of IL-6 and tumor necrosis factor (TNF)- $\alpha$  were measured using ELISA ( $n = 6$ ). Data are presented as the mean  $\pm$  SD. \* $P < 0.05$ , \*\* $P < 0.01$  (ANOVA).

We further examined changes in a panel of cytokines and chemokines in the sera using the Proteome Profiler Mouse Cytokine Array (R&D Systems). The serum levels of CCL2 and CXCL10 were increased in CP-treated mice followed by anti-CTLA-4 therapy (Fig. 5a). In ELISAs, CCL2 and CXCL10 serum levels were significantly increased in RENCA-bearing mice, but only when treated with both CP and anti-CTLA-4 therapy (Fig. 5b). Such changes were not observed in CT26-bearing or treated mice.

**Anti-CTLA-4 therapy accelerates CP-induced MDSCs in RENCA-bearing mice.** Chemokine ligand 2 traffics MDSCs that frequently increase in cancer-bearing hosts.<sup>(16–18)</sup> In addition, CCL2 is increased after CP treatment, thereby trafficking MDSCs from the bone marrow.<sup>(19)</sup> To this end, we examined MDSCs in the spleens of tumor-bearing and treated mice. MDSCs were evaluated according to their expression of Gr-1 and Ly6C among CD11b<sup>+</sup> cells. As shown in Figure 6(a), the combination of CP and anti-CTLA-4 therapy increased the percentage of CD11b<sup>+</sup> cells in the spleens of RENCA-bearing or CT26-bearing mice. Myeloid-derived suppressor cells are generally divided into monocytic CD11b<sup>+</sup> Gr-1<sup>low</sup> Ly6C<sup>+</sup> cells and

granulocytic CD11b<sup>+</sup> Gr-1<sup>+</sup> Ly6C<sup>-</sup> cells.<sup>(20,21)</sup> The staining and gating strategies used to examine myeloid cells are shown in Figure 6(b). As a result, a unique subset of CD11b<sup>+</sup> Gr-1<sup>+</sup> Ly6C<sup>high</sup> cells was detected. Given that the anti-Gr-1 mAb (clone RB6-8C5) binds to both Ly6G and Ly6C,<sup>(22)</sup> this Gr-1<sup>+</sup> Ly6C<sup>high</sup> cell population can be divided into monocytic cells. Therefore, in this study, we discriminated three subsets: monocytic CD11b<sup>+</sup> Gr-1<sup>-</sup> Ly6C<sup>+</sup> cells, monocytic CD11b<sup>+</sup> Gr-1<sup>+</sup> Ly6C<sup>high</sup> cells, and granulocytic CD11b<sup>+</sup> Gr-1<sup>+</sup> Ly6C<sup>low</sup> cells. Cyclophosphamide alone increased the percentage of CD11b<sup>+</sup> Gr-1<sup>+</sup> Ly6C<sup>high</sup> MDSCs in the spleens in both RENCA-bearing and CT26-bearing mice (Fig. 6b,c). Interestingly, additional anti-CTLA-4 therapy increased their percentage only in the spleen cells of RENCA-bearing mice. In RENCA-bearing mice, there was no significant difference in the percentage of CD4<sup>+</sup> Foxp3<sup>+</sup> Tregs in any group on day 6 after CP therapy (data not shown). We finally determined whether *in vivo* depletion of Gr-1<sup>+</sup> cells could affect the combination antitumor effects in RENCA-bearing mice. The result was that selective depletion of Gr-1<sup>+</sup> cells slightly enhanced the antitumor effect induced by the combination of CP and anti-CTLA-4 therapy (Figs 6d and S4).

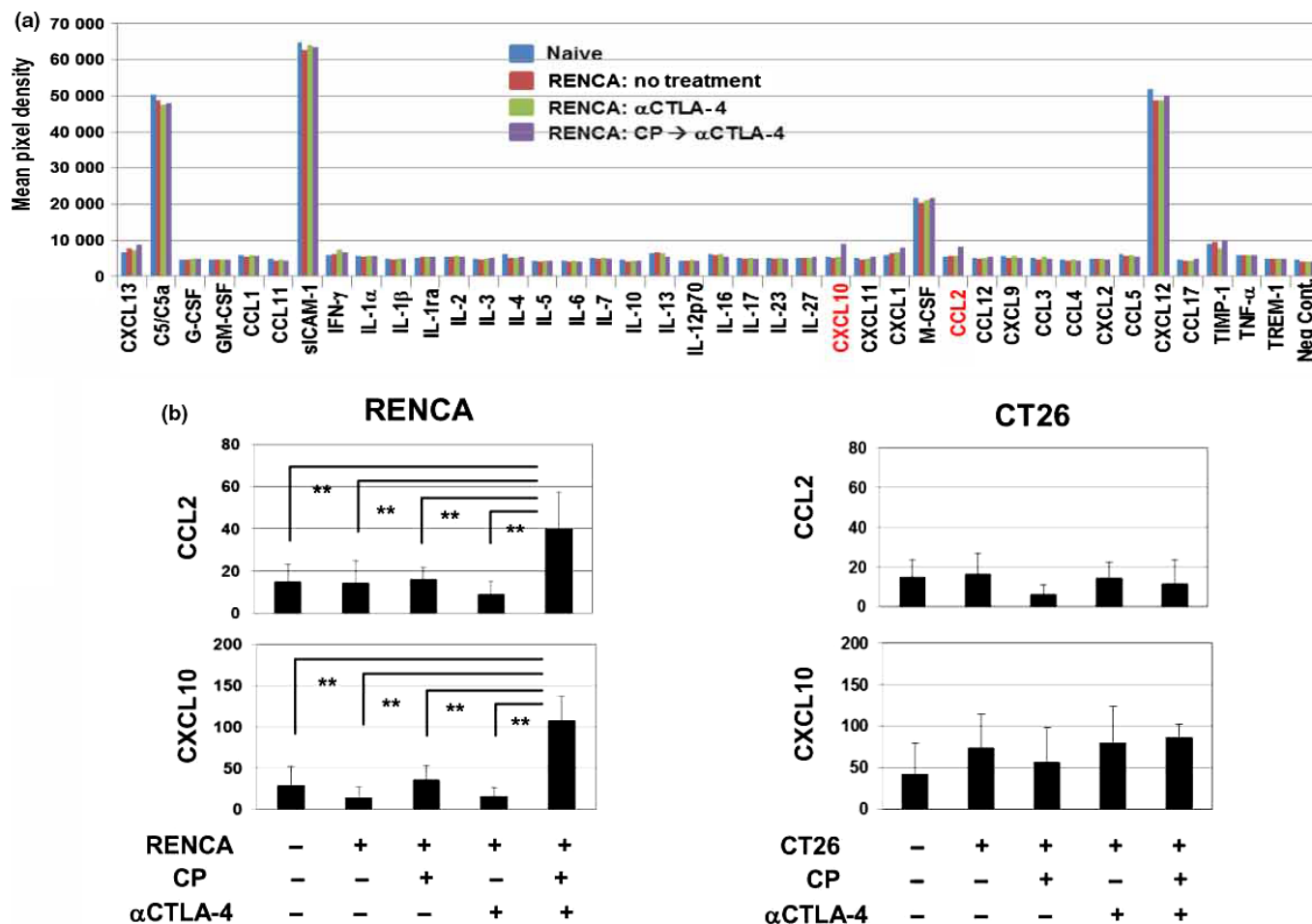


**Fig. 5.** Increased levels of serum chemokine ligand 2 (CCL2) and C-X-C motif chemokine 10 (CXCL10) in RENCA renal cell carcinoma-bearing mice that received combination therapy with cyclophosphamide (CP) and anti-CTL-associated protein 4 ( $\alpha$ CTLA-4) therapy. (a) Sera were collected and pooled from six mice on day 18 after tumor inoculation and the levels of cytokines and chemokines were evaluated using the Proteome Profiler Mouse Cytokine Array. (b) Serum levels (pg/mL) of CCL2 and CXCL10 were measured using ELISAs ( $n = 6$ ). Data are presented as the mean  $\pm$  SD.  $**P < 0.01$  (ANOVA). GM-CSF, granulocyte macrophage colony-stimulating factor; IFN- $\gamma$ ,  $\gamma$ -interferon; IL, interleukin; Neg Cont., negative control; sICAM-1, soluble intercellular adhesion molecules-1; TIMP-1, tissue inhibitors of metalloproteinase-1; TNF- $\alpha$ , tumor necrosis factor- $\alpha$ ; TREM-1, triggering receptor expressed on myeloid cell-1.

## Discussion

Although several reports have described the antitumor effects of combined anti-CTLA-4 therapy and chemotherapy,<sup>(23–25)</sup> we examined the antitumor effects of CP and anti-CTLA-4 therapy using two tumor murine models. Cyclophosphamide followed by anti-CTLA-4 therapy elicited a drastic regression of CT26 colon carcinoma, whereas the antitumor effects were weak in RENCA-bearing mice (Fig. 1c), prompting the question, why is the therapeutic efficacy different between the two models? One simple explanation is their different immunogenicities. In general, model antigen-expressing RENCA cells have been used to examine tumor-specific CTL responses,<sup>(26–28)</sup> suggesting their non/low immunogenicity. In contrast, numerous reports have revealed that CT26-specific CTLs are inducible, indicating their high immunogenicity. In support of this, we demonstrated CT26-specific CD8<sup>+</sup> T cells in cured mice (Fig. 1e,f). We also examined the antitumor effects of CP and anti-CTLA-4 therapy using poorly immunogenic B16 melanoma, although no tumor regression was observed (Fig. S2). These lines of evidence suggest that CP followed by anti-CTLA-4 therapy is a promising regimen to treat immunogenic tumors but not non/low immunogenic

tumors. Alternatively, there may be other reasons for its insufficient therapeutic efficacy in RENCA-bearing mice. RENCA cells produced higher levels of IL-6 and TNF- $\alpha$  *in vitro*, and serum levels of IL-6 were higher in RENCA-bearing mice compared to CT26-bearing mice (Fig. 4b,c). Given that these inflammatory cytokines induce cachexia at high levels,<sup>(15)</sup> an increase in IL-6 might aggravate the immune competence of RENCA-bearing mice and decrease their responsiveness to combination therapy. In addition, as discussed below, the accelerated increase in MDSCs after anti-CTLA-4 therapy may account for its insufficient therapeutic efficacy in RENCA-bearing mice.

We tested the optimal combination regimen of CP and ICB therapy using an immunogenic CT26 model. Cyclophosphamide before anti-CTLA-4 therapy exerted a more efficient antitumor effect than CP after anti-CTLA-4 therapy (Fig. 2a). This result may be because cytotoxic CP was given on day 12 in the former regimen but injected on day 15 in the latter. It is plausible that a larger tumor (on day 15) is more resistant to CP than a smaller tumor (on day 12). However, CP after anti-CTLA-4 therapy induced apoptosis in tumor-specific CD8<sup>+</sup> T cells in draining LNs compared to when the order was

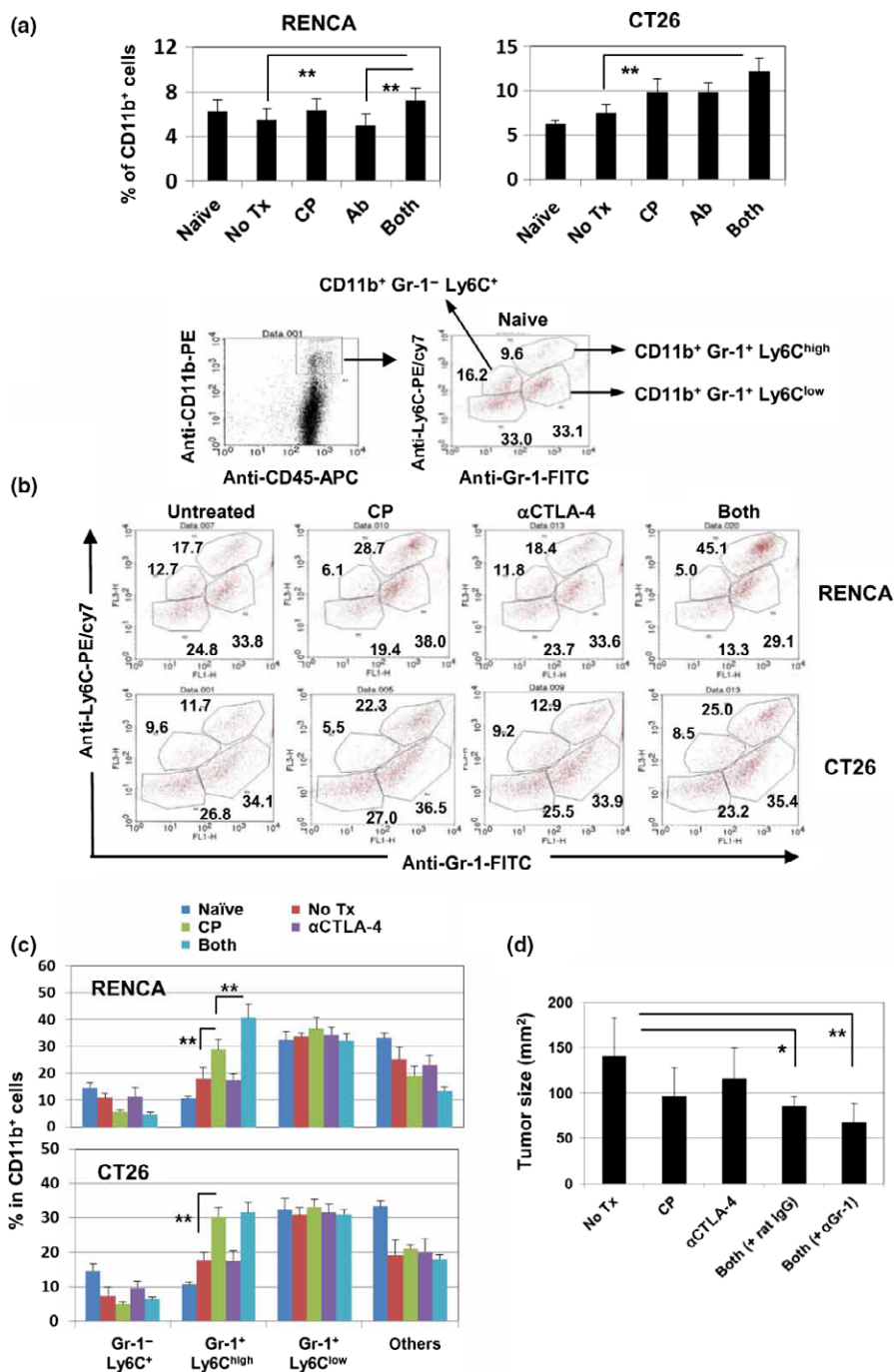


**Fig. 6.** Anti-CTL-associated protein 4 (CTLA-4) therapy following cyclophosphamide (CP) elevates CP-induced myeloid-derived suppressor cells in RENCA renal cell carcinoma-bearing mice. (a) Spleens were harvested on day 18 after tumor inoculation and analyzed by flow cytometry. The spleen cell numbers and percentages of CD11b<sup>+</sup> cells are shown (n = 6). Data are presented as the mean ± SD. \*\*P < 0.01 (ANOVA). (b) Staining strategy and representative results. Numbers represent the percentage of each subset. (c) Percentage of each subset in CD11b<sup>+</sup> cells is shown (n = 6). Data are presented as the mean ± SD. \*\*P < 0.01 (ANOVA). (d) BALB/c mice were inoculated s.c. with RENCA cells (1 × 10<sup>6</sup>). Mice were injected i.p. with CP (100 mg/kg) on day 12 followed by anti-CTLA-4 mAb (100 μg) or hamster IgG on days 13 and 15. In the indicated groups, anti-Gr-1 mAb (100 μg) or rat IgG was given i.p. on days 15 and 17. Tumor size (on day 29) are presented as the mean ± SD (n = 6). \*P < 0.05, \*\*P < 0.01 (ANOVA). APC, allophycocyanin; PE, phycoerythrin; Tx, treatment.

reversed (Fig. 2b,c). Given that CP kills proliferating cancer cells, this drug could also destroy tumor-specific T cells that are reactivated and proliferating after anti-CTLA-4 therapy. Consistent with this hypothesis, alloantigen-stimulated and proliferating T cells can be preferentially destroyed by a subsequent injection of CP.<sup>(29)</sup> This negative property of CP should be considered when combined with ICB therapy.

Cyclophosphamide induces PD-L1-expressing MDSCs, indicating its therapeutic benefits in combination with anti-PD-1/PD-L1 therapy.<sup>(30)</sup> In this regard, the combination of CP and anti-PD-1 therapy was not as effective in CT26-bearing mice compared with CP and anti-CTLA-4 therapy (Fig. 3). With respect to the mechanisms underlying this difference, we hypothesize the following scenario. Treatment with CP

mitigates Treg-mediated immunosuppression<sup>(10,11)</sup> and induces immunogenic cancer cell death.<sup>(9)</sup> Next, DCs that uptake released tumor antigens move to the draining LNs where DCs prime tumor-specific T cells. Primed and activated T cells express CTLA-4 molecules, but anti-CTLA-4 mAbs effectively relieve immune exhaustion. In addition, anti-CTLA-4 therapy attenuates Treg-mediated immunosuppression.<sup>(31)</sup> Thereafter, effectively activated antitumor T cells in draining LNs migrate into tumor sites and exert their cytotoxic activity against cancer cells. The repeated uptake of tumor antigens by DCs from destroyed cancer cells triggers the priming of tumor-specific CTLs at draining LNs. Considering the significance of the cancer-immunity cycle in anticancer immunotherapy,<sup>(32)</sup> the combination of CP and anti-CTLA-4 therapy may effectively rotate this cycle. Conversely, anti-PD-1 therapy mainly exerts its effects at tumor sites where CD8<sup>+</sup> T cells kill cancer cells.<sup>(7)</sup> The priming of tumor-specific CTLs at draining LNs must not be sufficient when CP is combined with anti-PD-1 therapy, suggesting that the cancer-immunity cycle does not rotate well.

In the RENCA model, anti-CTLA-4 therapy led to a reduction in body weight, as a representative symptom of IrAEs, but pretreatment with CP relieved this effect (Fig. 4a). Given that either CP or anti-CTLA-4 therapy alone significantly decreased serum IL-6 and TNF- $\alpha$  levels (Fig. 4c) but that the reduction in body weight was not recovered, decreases in IL-6 and TNF- $\alpha$  cannot explain why pre-injection of CP relieved the reduction in body weight in RENCA-bearing and anti-CTLA-4-treated mice. Interestingly, both CCL2 and CXCL10 were elevated in combination therapy-treated RENCA-bearing mice (Fig. 5). Intriguingly, it has been known that CCL2 increases after CP treatment, thereby leading to trafficking of MDSCs from the bone marrow.<sup>(19)</sup> Therefore, we hypothesized that the increase in immunosuppressive MDSCs after combination therapy mitigated the reduction in body weight in anti-CTLA-4-treated RENCA-bearing mice. However, the depletion of Gr-1<sup>+</sup> cells failed to replicate the reduction in body weight observed in anti-CTLA-4-treated RENCA-bearing mice (data not shown). At present, we cannot confirm the mechanisms involved. However, a recent report revealed that the antitumor effects and IrAEs after anti-CTLA-4 therapy are influenced by intestinal microbiota.<sup>(33)</sup> Further studies are required to elucidate the precise mechanisms involved.

Chemokines CCL2 and CXCL10 were elevated in combination therapy-treated RENCA-bearing mice but not in CT26-bearing mice (Fig. 5b). These chemokines are known to play multiple roles in antitumor immunity and immunotherapy. High-dose CP increases the circulating levels of type I interferon-induced cytokines, including CXCL10, and inflammatory mediators, including CCL2.<sup>(34,35)</sup> Chemokine ligand 2 is secreted in response to apoptotic bodies in the "sterile" inflammatory response.<sup>(36)</sup> C-X-C motif chemokine 10 is required for IL-12-mediated regression of RENCA.<sup>(37)</sup> It seems that CXCL10 and CCL2 are antitumor and tumor-promoting chemokines, respectively.<sup>(38,39)</sup> Of note, CCL2 regulates the recruitment of myeloid cells into tumors.<sup>(16,17,40)</sup> Additionally, several reports have indicated that CP induces immunosuppressive MDSCs not only in tumor-bearing mice but also in naïve mice.<sup>(30)</sup> These results suggest that CP triggers a surge of inflammatory cytokines and chemokines to elicit homeostatic proliferation and to recover immune cells. Alternatively, MDSCs can also be increased after treatment with other anticancer drugs, such as melphalan and doxorubicin, radiotherapy, and adoptive T-cell therapy.<sup>(30,31,41,42)</sup> Presumably,

increased MDSCs after these therapies may exert a counter-regulatory role in preventing excessive inflammatory and immune responses after cell death.

As the combination of CP and anti-CTLA-4 therapy increased the serum levels of CCL2 in RENCA-bearing mice, we examined MDSCs in the spleen. Monocytic CD11b<sup>+</sup> Gr-1<sup>+</sup> Ly6C<sup>high</sup> MDSCs were increased in both RENCA- and CT26-bearing mice 6 days after CP monotherapy (Fig. 6b,c), consistent with a previous report.<sup>(30)</sup> Importantly, additional anti-CTLA-4 therapy escalated the percentage only in RENCA-bearing mice. This increase seems to depend on CCL2. However, it remains to be determined whether CP-induced MDSCs are the same as tumor-derived MDSCs. As mentioned above, CP can increase MDSCs in naïve mice.<sup>(30)</sup> In this regard, previous reports have suggested that the CP-induced MDSC population is not identical to that in the tumor-bearing state;<sup>(43)</sup> both are immunosuppressive monocytic MDSCs, whereas CP-induced MDSCs exert immunosuppression, mainly through nitric oxide and reactive oxygen species.<sup>(44)</sup> To overcome MDSC-mediated immunosuppression, several methods have been proposed. Chemotherapeutic drugs, such as gemcitabine and 5-fluorouracil, can decrease MDSCs.<sup>(12,13)</sup> The combination of CP and gemcitabine can simultaneously mitigate Tregs and MDSCs.<sup>(45)</sup> In addition, anti-CCR2 agents, all-trans retinoic acid, and the DNA-demethylating agent 5-azacytidine have been reported to prevent an increase in CP-induced MDSCs.<sup>(42,43,46)</sup> These agents could thus prevent an emergence of counter-regulatory MDSCs and thereby augment its therapeutic efficacy.

In conclusion, our results reveal the contrasting effects of CP on anti-CTLA-4 therapy in two mouse tumor models. These findings provide insight into effective antitumor therapies in which ICB therapy is combined with chemotherapeutic drugs.

## Acknowledgments

We thank Ms. Tamami Moritani for her technical assistance. This study was supported in part by the Japan Society for the Promotion of Science (KAKENHI grant no. 17K07217 to M.H.) and from the Shimane University "SUIGANN" Project.

## Disclosure Statement

The authors have no conflict of interest.

## Abbreviations

APC	allophycocyanin
CCL2	chemokine ligand 2
CP	cyclophosphamide
CTLA-4	CTL-associated protein 4
CXCL10	C-X-C motif chemokine 10
DC	dendritic cell
Gr-1	granulocyte-differentiation antigen-1
ICB	immune checkpoint blockade
IL	interleukin
IrAE	immune-related adverse event
LN	lymph node
MDSC	myeloid-derived suppressor cell
PD-1	programmed cell death-1
PD-L1	programmed cell death ligand-1
PE	phycoerythrin
TNF- $\alpha$	tumor necrosis factor- $\alpha$
Treg	regulatory T cell

## References

- Topalian SL, Taube JM, Anders RA, Pardoll DM. Mechanism-driven biomarkers to guide immune checkpoint blockade in cancer therapy. *Nat Rev Cancer* 2016; **16**: 275–87.
- Ott PA, Hodi FS, Robert C. CTLA-4 and PD-1/PD-L1 blockade: new immunotherapeutic modalities with durable clinical benefit in melanoma patients. *Clin Cancer Res* 2013; **19**: 5300–9.
- Sharma P, Allison JP. Immune checkpoint targeting in cancer therapy: toward combination strategies with curative potential. *Cell* 2015; **16**: 205–14.
- Pfirschke C, Engblom C, Rickelt S *et al.* Immunogenic chemotherapy sensitizes tumors to checkpoint blockade therapy. *Immunity* 2016; **44**: 343–54.
- Michot JM, Bigenwald C, Champiat S *et al.* Immune-related adverse events with immune checkpoint blockade: a comprehensive review. *Eur J Cancer* 2016; **54**: 139–48.
- He XS, Gershwin ME, Ansari AA. Checkpoint-based immunotherapy for autoimmune diseases - Opportunities and challenges. *J Autoimmun* 2017; **79**: 1–3.
- Postow MA, Callahan MK, Wolchok JD. Immune checkpoint blockade in cancer therapy. *J Clin Oncol* 2015; **33**: 1974–82.
- Galluzzi L, Buqué A, Kepp O, Zitvogel L, Kroemer G. Immunological effects of conventional chemotherapy and targeted anticancer agents. *Cancer Cell* 2015; **28**: 690–714.
- Kroemer G, Galluzzi L, Kepp O, Zitvogel L. Immunogenic cell death in cancer therapy. *Annu Rev Immunol* 2013; **31**: 51–72.
- Sistigu A, Viaud S, Chaput N, Bracci L, Proietti E, Zitvogel L. Immunomodulatory effects of cyclophosphamide and implementations for vaccine design. *Semin Immunopathol* 2011; **33**: 369–83.
- Ghiringhelli F, Larmonier N, Schmitt E *et al.* CD4+CD25+ regulatory T cells suppress tumor immunity but are sensitive to cyclophosphamide which allows immunotherapy of established tumors to be curative. *Eur J Immunol* 2004; **34**: 336–44.
- Suzuki E, Kapoor V, Jassar AS, Kaiser LR, Albelda SM. Gemcitabine selectively eliminates splenic Gr-1+CD11b+ myeloid suppressor cells in tumor-bearing animals and enhances antitumor immune activity. *Clin Cancer Res* 2005; **11**: 6713–21.
- Vincent J, Mignot G, Chalmin F *et al.* 5-Fluorouracil selectively kills tumor-associated myeloid-derived suppressor cells resulting in enhanced T cell-dependent antitumor immunity. *Cancer Res* 2010; **70**: 3052–61.
- Huang AY, Gulden PH, Woods AS *et al.* The immunodominant major histocompatibility complex class I-restricted antigen of a murine colon tumor derives from an endogenous retroviral gene product. *Proc Natl Acad Sci USA* 1996; **93**: 9730–5.
- Cahlin C, Körner A, Axelsson H, Wang W, Lundholm K, Svanberg E. Experimental cancer cachexia: the role of host-derived cytokines interleukin (IL)-6, IL-12, interferon-gamma, and tumor necrosis factor alpha evaluated in gene knockout, tumor-bearing mice on C57 Bl background and eicosanoid-dependent cachexia. *Cancer Res* 2000; **60**: 5488–93.
- Hartwig T, Montinaro A, von Karstedt S *et al.* The TRAIL-induced cancer secretome promotes a tumor-supportive immune microenvironment via CCR2. *Mol Cell* 2017; **65**: 730–42.
- Chang AL, Miska J, Wainwright DA *et al.* CCL2 produced by the glioma microenvironment is essential for the recruitment of regulatory T cells and myeloid-derived suppressor cells. *Cancer Res* 2016; **76**: 5671–82.
- Ostrand-Rosenberg S, Sinha P. Myeloid-derived suppressor cells: linking inflammation and cancer. *J Immunol* 2009; **182**: 4499–5060.
- Ding ZC, Munn DH, Zhou G. Chemotherapy-induced myeloid suppressor cells and antitumor immunity: the Janus face of chemotherapy in immunomodulation. *Oncimmunology* 2014; **3**: e954471.
- Youn JI, Nagaraj S, Collazo M, Gabrilovich DI. Subsets of myeloid-derived suppressor cells in tumor-bearing mice. *J Immunol* 2008; **181**: 5791–802.
- Sinha P, Parker KH, Horn L, Ostrand-Rosenberg S. Tumor-induced myeloid-derived suppressor cell function is independent of IFN- $\gamma$  and IL-4R $\alpha$ . *Eur J Immunol* 2012; **42**: 2052–9.
- Daley JM, Thomay AA, Connolly MD, Reichner JS, Albina JE. Use of Ly6G-specific monoclonal antibody to deplete neutrophils in mice. *J Leukoc Biol* 2008; **83**: 64–70.
- Jure-Kunkel M, Masters G, Girit E *et al.* Synergy between chemotherapeutic agents and CTLA-4 blockade in preclinical tumor models. *Cancer Immunol Immunother* 2013; **62**: 1533–45.
- Lesterhuis WJ, Salmons J, Nowak AK *et al.* Synergistic effect of CTLA-4 blockade and cancer chemotherapy in the induction of anti-tumor immunity. *PLoS ONE* 2013; **8**: e61895.
- Parra K, Valenzuela P, Lerma N *et al.* Impact of CTLA-4 blockade in conjunction with metronomic chemotherapy on preclinical breast cancer growth. *Br J Cancer* 2017; **116**: 324–34.
- Basingab FS, Ahmadi M, Morgan DJ. IFN $\gamma$ -dependent interactions between ICAM-1 and LFA-1 counteract prostaglandin E2-mediated inhibition of anti-tumor CTL responses. *Cancer Immunol Res* 2016; **4**: 400–11.
- Shanker A, Brooks AD, Jacobsen KM *et al.* Antigen presented by tumors *in vivo* determines the nature of CD8 + T-cell cytotoxicity. *Cancer Res* 2009; **69**: 6615–23.
- Sloots A, Mastini C, Rohrbach F *et al.* DNA vaccines targeting tumor antigens to B7 molecules on antigen-presenting cells induce protective antitumor immunity and delay onset of HER-2/Neu-driven mammary carcinoma. *Clin Cancer Res* 2008; **14**: 6933–43.
- Eto M, Mayumi H, Tomita Y, *et al.* Specific destruction of host-reactive mature T cells of donor origin prevents graft-versus-host disease in cyclophosphamide-induced tolerant mice. *J Immunol* 1991; **146**: 1402–9.
- Ding ZC, Lu X, Yu M *et al.* Immunosuppressive myeloid cells induced by chemotherapy attenuate antitumor CD4+ T-cell responses through the PD-1-PD-L1 axis. *Cancer Res* 2014; **74**: 3441–53.
- Ménard C, Ghiringhelli F, Roux S *et al.* Ctl4-4 blockade confers lymphocyte resistance to regulatory T-cells in advanced melanoma: surrogate marker of efficacy of tremelimumab? *Clin Cancer Res* 2008; **14**: 5242–9.
- Chen DS, Mellman I. Oncology meets immunology: the cancer-immunity cycle. *Immunity* 2013; **39**: 1–10.
- Dubin K, Callahan MK, Ren B *et al.* Intestinal microbiome analyses identify melanoma patients at risk for checkpoint-blockade-induced colitis. *Nat Commun* 2016; **7**: 10391.
- Moschella F, Valentini M, Aricò E *et al.* Unraveling cancer chemoimmunotherapy mechanisms by gene and protein expression profiling of responses to cyclophosphamide. *Cancer Res* 2011; **71**: 3528–39.
- Moschella F, Torelli GF, Valentini M *et al.* Cyclophosphamide induces a type I interferon-associated sterile inflammatory response signature in cancer patients' blood cells: implications for cancer chemoimmunotherapy. *Clin Cancer Res* 2013; **19**: 4249–61.
- Berda-Haddad Y, Robert S *et al.* Sterile inflammation of endothelial cell-derived apoptotic bodies is mediated by interleukin-1 $\alpha$ . *Proc Natl Acad Sci USA* 2011; **108**: 20684–9.
- Tannenbaum CS, Tubbs R, Armstrong D, Finke JH, Bukowski RM, Hamilton TA. The CXC chemokines IP-10 and Mig are necessary for IL-12-mediated regression of the mouse RENCA tumor. *J Immunol* 1998; **161**: 927–32.
- Sistigu A, Yamazaki T, Vacchelli E *et al.* Cancer cell-autonomous contribution of type I interferon signaling to the efficacy of chemotherapy. *Nat Med* 2014; **20**: 1301–9.
- McClellan JL, Davis JM, Steiner JL *et al.* Linking tumor-associated macrophages, inflammation, and intestinal tumorigenesis: role of MCP-1. *Am J Physiol Gastrointest Liver Physiol* 2012; **303**: G1087–95.
- Popivanova BK, Kostadinova FI, Furuichi K *et al.* Blockade of a chemokine, CCL2, reduces chronic colitis-associated carcinogenesis in mice. *Cancer Res* 2009; **69**: 7884–92.
- Kodumudi KN, Weber A, Sarnaik AA, Pilon-Thomas S. Blockade of myeloid-derived suppressor cells after induction of lymphopenia improves adoptive T cell therapy in a murine model of melanoma. *J Immunol* 2012; **189**: 5147–54.
- Hosoi A, Matsushita H, Shimizu K *et al.* Adoptive cytotoxic T lymphocyte therapy triggers a counter-regulatory immunosuppressive mechanism via recruitment of myeloid-derived suppressor cells. *Int J Cancer* 2014; **134**: 1810–22.
- Mikyšková R, Indrová M, Polláková V, Bieblová J, Símová J, Reiniš M. Cyclophosphamide-induced myeloid-derived suppressor cell population is immunosuppressive but not identical to myeloid-derived suppressor cells induced by growing TC-1 tumors. *J Immunother* 2012; **35**: 374–84.
- Sevko A, Sade-Feldman M, Kanterman J *et al.* Cyclophosphamide promotes chronic inflammation-dependent immunosuppression and prevents antitumor response in melanoma. *J Invest Dermatol* 2013; **133**: 1610–19.
- Tongu M, Harashima N, Monma H *et al.* Metronomic chemotherapy with low-dose cyclophosphamide plus gemcitabine can induce anti-tumor T cell immunity *in vivo*. *Cancer Immunol Immunother* 2013; **62**: 383–91.
- Mikyšková R, Indrová M, Vlčková V *et al.* DNA demethylating agent 5-aza-cytidine inhibits myeloid-derived suppressor cells induced by tumor growth and cyclophosphamide treatment. *J Leukoc Biol* 2014; **95**: 743–53.

## Supporting Information

Additional Supporting Information may be found online in the supporting information tab for this article:

**Fig. S1.** Effect of several doses of cyclophosphamide (CP) on regulatory T cells (Tregs) in tumor tissues.

**Fig. S2.** Antitumor effects of cyclophosphamide (CP) and anti-CTL-associated protein 4 (CTLA-4) therapy on established B16 melanoma.

**Fig. S3.** Induction of CT26-specific CTLs following cyclophosphamide (CP) and anti-CTL-associated protein 4 (CTLA-4) therapy.

**Fig. S4.** Effects of *in vivo* depletion of Gr-1<sup>+</sup> cells in RENCA-bearing mice treated with cyclophosphamide (CP) and anti-CTL-associated protein 4 (CTLA-4) mAb.